On the Design Conditions of Planar Parallel Manipulators in Near-Singular Configurations

Sébastien Briot, Victor Glazunov, Vigen Arakelian

On the Design Conditions of Planar Parallel Manipulators in Near-Singular Configurations

S. Briot*
IRCCyN – CNRS
Nantes, France

V. Glazunov†
Russian Academy of Sciences
Moscow, Russia

V. Arakelian‡
INSA
Rennes, France

Abstract— *Singularity is a major problem for parallel manipulators as it causes severe problems: uncontrollable or unstable motions, loss of stiffness, infinite forces/torques in actuated joints, and possibility of a breakdown. Many studies have been devoted to these problems. In particular, various criteria for measuring the closeness to singularities have been proposed. They are based on the limitation of the values of the input force/torque, pressure angle, natural frequency, etc. The present paper expands the previous work by incorporating a new criterion into mentioned problem, which allows the limitation of the reaction in passive joints. For this purpose, a new approach is developed, which shows that for given external force and moment applied on the platform, the reactions in passive joints depend not only on the pressure angle but also the position of the instantaneous centre of rotation of the platform. The developed approach is not only an effective way to reduce computation time but also to give a qualitative and geometrical interpretation of the problem. The suggested procedure for the determination of the reachable manipulator workspace taking into account the admissible reactions in passive joints is illustrated via a planar 3-RRR parallel manipulator.*

Keywords: design, effort transmission, instantaneous centre of rotation, planar parallel robots, pressure angle, singularities.

I Introduction

It is well known that a parallel manipulator at a singular configuration can gain one or more degrees of freedom. Moreover, at such a configuration, it cannot be controlled, and it can have infinite force/torque in actuated joints, as well as infinite reactions in passive joints, leading to a manipulator breakdown. Therefore the singular configurations and the properties of parallel manipulators close to these configurations have been studied. The singularity analysis of parallel manipulators have been carried out from kinematic [1-5], kinetostatic [6-8] and dynamic points of view [9-11]. The task of avoiding singular configurations raises the question of how one has to stay away from singular configurations. From this point of view, different criteria and several approaches have been proposed. The optimization under constraints has been used [12] to determine the linear complex that is closest to a singularity. This methodology was applied to describe the instantaneous behavior near singularities [13]. The optimization under constraints was also adapted in order to generalize the concept of center-of-compliance [14, 15]. The dexterity and conditioning indices were also proposed [16, 17]. These indices are based on the Jacobian matrix or its "norm", which relate the actuator velocities (efforts, resp.) to the platform twist (wrench, resp.) by the following relations:

$$\mathbf{t} = \mathbf{J}\dot{\mathbf{q}} \quad \text{and} \quad \mathbf{w} = \mathbf{J}^{-T}\boldsymbol{\tau} \tag{1}$$

where $\mathbf{J}$ is the Jacobian matrix, $\mathbf{t}$ the platform twist, $\dot{\mathbf{q}}$ the input velocities, $\boldsymbol{\tau}$ the actuator efforts, and $\mathbf{w}$ the wrench applied on the platform.

However, it is known that because of the non homogeneity of the terms of the Jacobian matrix, the previous indices are not well appropriated for mechanisms having both translational and rotational degrees of freedom (DOF). Moreover, as they are based on the Euclidian norm of the input vector ($\|\dot{\mathbf{q}}\|$ or $\|\boldsymbol{\tau}\|$ being considered equal to 1), while it is clear that each actuator may have a velocity or an effort comprised between a minimal and a maximal value ($\dot{q}_i \in [-\dot{q}_i^{\max}, \dot{q}_i^{\max}]$ and $\tau_i \in [-\tau_i^{\max}, \tau_i^{\max}]$, $\dot{q}_i$ and τ_i being the velocity and effort of actuator i), they do not take into account the 'technological reality' of the mechanism.

In order to overcome these drawbacks, in [8] it is proposed to characterize the force workspace of robots, which is the workspace for which, considering a given fixed wrench applied on the platform, the actuator efforts are always comprised in the interval $[-\tau_i^{\max}, \tau_i^{\max}]$. However, this workspace depends on the given direction and norm of the external wrench and will change if another wrench is considered. Moreover, for many robot applications, the wrench direction is not known, contrary to its norm. Therefore, in [18], a way to compute the maximal workspace taking into account the actuator effort limitations for a given norm of the external wrench was proposed. This approach is based on the computation of the transmission factors of matrix $\mathbf{J}^{-T}$, which are

* Sebastien.Briot@irccyn.ec-nantes.fr
† vaglznv@mail.ru
‡ vigen.arakelyan@insa-rennes.fr
[1]13th World Congress in Mechanism and Machine Science, Guanajuato, México, 19-25 June, 2011

obtained geometrically through the mapping of a cube by the Jacobian matrix.

The main drawback of the last two approaches appears in the fact that they analyze the mechanism breakdown by considering input torque limitations only. However, it can exist such poses of the manipulator close to the singularity for which the limitations of input torques can be satisfied but where the reactions in passive joints are not admissible. To have a better understanding of this fact, let us consider a simple example. For the planar 5*R* manipulator close to the singularity (Fig. 1), a small effort **w** applied on the end-effector will create a large reaction $\mathbf{R_1}$ in the passive joint *B*. But in this pose, the actuator torques τ_1 will stay under acceptable values, as it depends only on the small component $\mathbf{F_1}$ of the reaction $\mathbf{R_1}$.

Thus we see that the limitation of the passive joints' reactions is also an important consideration. It is a complementary criterion for measuring closeness to singularity. The most trivial way to compute the maximal passive joint reactions is to apply the Newton-Euler theorem to the manipulator platform and, by variation of the force vector directions and moment values, to compute the joint reactions. However, this is a complicated way which requires considerably huge computation time.

Therefore, in this paper a new method for obtaining the maximal efforts in passive joints taking into account the norm of the external wrench applied on the platform of planar parallel manipulator is proposed. It will be shown that, for a given ratio between the norm of the external wrench and of the maximal admissible effort into the passive joints, the mechanical breakdown can be avoided if the pressure angle and the minimal distance between the considered passive joint and the platform instantaneous axis of rotation are bounded. The developed approach is not only an effective way to reduce computation time but also to give a qualitative and geometrical interpretation of the problem.

II. A new criterion for evaluation of the passive joints efforts

For any planar manipulator, the forces $\mathbf{R}_i$ transmitted by the legs through the passive joints linked to the platform (Fig. 2) can be related to the external wrench $\mathbf{w}^T = [\mathbf{f}^T, m]^T$ (**f** is the external force, and *m* the scalar value of the external moment applied on the platform) using the Newton-Euler theorem at any point *Q*:

$$\mathbf{f} = -\sum_{i=1}^{3} \mathbf{R}_i \quad \text{and} \quad m = -\sum_{i=1}^{3} \overline{\mathbf{d}}_{QBi}^T \mathbf{R}_i \tag{2}$$

where $\overline{\mathbf{d}}_{QBi}^T = [-y_{QBi}, x_{QBi}]$, with x_{QBi} and y_{QBi} are the coordinates of vector $\mathbf{QB}_i$ along ***x*** and ***y*** axes. Considering that $\mathbf{R}_i = R_i\, \mathbf{r}_i$, where $\|\mathbf{R}_i\| = R_i$, and applying the Newton-Euler theorem at point B_1, it comes that:

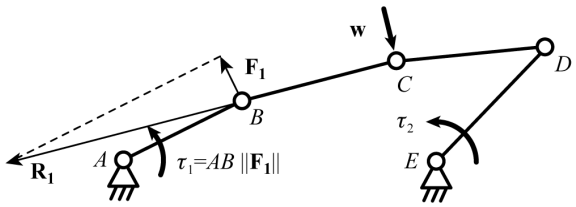

Fig. 1. Planar 5*R* manipulator close to the Type 2 singular pose.

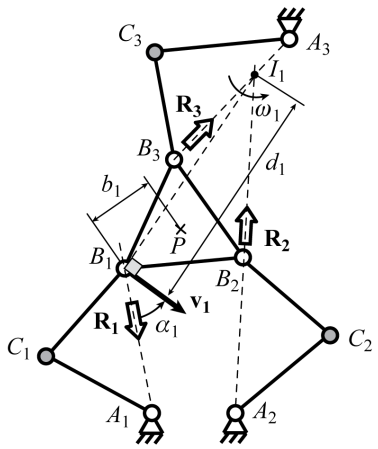

Fig. 2. Determination of the pressure angle for the planar 3-*RRR* robot.

$$\mathbf{w} = -\begin{bmatrix} \mathbf{r_1} & \mathbf{r_2} & \mathbf{r_3} \\ 0 & \overline{\mathbf{d}}_{B_1B_2}^T \mathbf{r_2} & \overline{\mathbf{d}}_{B_1B_3}^T \mathbf{r_3} \end{bmatrix} \begin{bmatrix} R_1 \\ R_2 \\ R_3 \end{bmatrix} \tag{3}$$

$$= -\begin{bmatrix} \mathbf{f_1} & \mathbf{f_2} & \mathbf{f_3} \end{bmatrix} \mathbf{R} = -\mathbf{A}^T \mathbf{R}$$

$\mathbf{f}_i^T = \left[\mathbf{r}_i^T, \overline{\mathbf{d}}_{B_iB_i}^T \mathbf{r}_i \right]$ being a unit screw corresponding to the direction of the wrench applied by the actuators on the platform.

Matrix **A** used in equation (3) is defined in [1] as the parallel Jacobian matrix than can be found through the differentiation of the loop closure equations of the robot with respect to the platform coordinates. As a result, this matrix is always invertible if the robot is not in a Type 2 singularity.

The reactions **R** of the passive joints can be found from (3):

$$\mathbf{R} = -\mathbf{A}^{-T} \mathbf{w}\,, \tag{4}$$

where matrix $\mathbf{A}^{-1}$ can be expressed in the form:

$$\mathbf{A}^{-1} = \begin{bmatrix} \mathbf{t_1} & \mathbf{t_2} & \mathbf{t_3} \end{bmatrix}, \text{ with } \mathbf{t}_i^T = [\mathbf{v}_i^T, \omega_i] \tag{5}$$

where $\mathbf{t}_i$ is a screw collinear to the twist of the platform expressed at point B_i when leg *i* is disconnected, $\mathbf{v}_i$ is the translational velocity of point B_i, and ω_i the platform rotational velocity [7] (Fig. 2). On this picture, point I_1 corresponds to the instantaneous centre of rotation of the platform when leg 1 is disconnected.

Taking into account that $\mathbf{A}^T\mathbf{A}^{-T} = \mathbf{I}$, we obtain: $\mathbf{f_1}^T \mathbf{t_1} = \mathbf{r_1}^T \mathbf{v_1} = 1$.

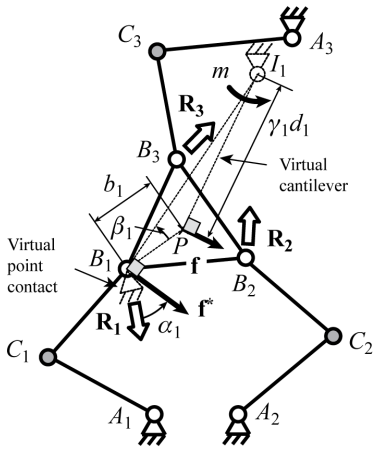

Fig. 3. Instantaneous system equivalent to the planar 3- *RRR* robot platform.

It was shown in [7] that the pressure angle of the leg 1, depicted as α_1 (see Fig. 2), may be expressed as the acute angle between the directions of vectors $\mathbf{r}_1$ and $\mathbf{v}_1$. Therefore:

$$\left|\mathbf{r_1}^T\mathbf{v_1}\right| = \|\mathbf{r_1}\|\|\mathbf{v_1}\|\cos\alpha_1 \text{, i.e. } \cos\alpha_1 = \frac{\left|\mathbf{r_1}^T\mathbf{v_1}\right|}{\|\mathbf{r_1}\|\|\mathbf{v_1}\|} \qquad (6)$$

By definition, $\mathbf{r_1}$ is a unit vector. As a result, $\|\mathbf{v_1}\| = (\cos\alpha_1)^{-1}$.

For a rigid body in a planar displacement, it is known that the norm of the translational velocity $\mathbf{v_Q}$ of any point Q is equal to the product of the angular velocity absolute value by the distance between Q and the instantaneous centre of rotation of the body (denoted as I). Thus, we have $\|\mathbf{v_1}\| = d_1|\omega_1|$, where d_1 is the distance from the platform instantaneous centre of rotation I_1 to point B_1 (Fig. 2).

Developing (4), it comes that:

$$R_1 = -\left(\mathbf{v_1}^T\mathbf{f} + \omega_1(m + \bar{\mathbf{d}}_{B1P}^T\mathbf{f})\right) = -\left((\mathbf{v_1}^T + \omega_1\bar{\mathbf{d}}_{B1P}^T)\mathbf{f} + \omega_1 m\right).$$

For a given norm f of the external force $\mathbf{f}$ and a given value m of the external moment, and for any direction of vector $\mathbf{f}$, the maximal value $R_{1\max}$ of R_1 appears when

$$R_{1\max} = \max_{\mathbf{f},m}(R_1) = f\sqrt{\|\mathbf{v_1}\|^2 + (\omega_1 b_1)^2 - 2\|\mathbf{v_1}\|\left|\omega_1 b_1\right|\cos\beta_1} + \left|\omega_1 m\right| \qquad (7)$$

where b_1 is the distance between the application point of the external wrench, denoted as P, and point B_1. β_1 is the angle between vectors $\mathbf{v_1}$ and $-\omega_1\bar{\mathbf{d}}_{B1P}$. For a numerical computation of the joint reactions, using (7) could be sufficient, as all of these parameters can be defined via matrix $\mathbf{A}$ and the mechanism geometry. But, it will be shown below that we can go deeper in the analysis using the pressure angle α_1 and the distance d_1. These indices will give valuable insights for the effort transmission inside of the mechanism.

Transforming expression (7) taking exp. (6) into account, and generalizing the approach to the other legs, we obtain the maximal value $R_{i\max}$ of the platform joint reaction at B_i (i = 1 to 3)

$$R_{i\max} = \frac{\gamma_i f + \left|m\right|/d_i}{\cos\alpha_i} \qquad (8)$$

where $\gamma_i = \sqrt{1 + (b_i/d_i)^2 - 2\cos\beta_i\, b_i/d_i}$, d_i is the distance between point B_i and the instantaneous centre of rotation of the platform when leg i is disconnected, α_i is the pressure angle of the leg i, b_i is the distance between P and B_i, and β_i is the angle between vectors $\mathbf{v}_i$ and $-\omega_i\bar{\mathbf{d}}_{BiP}$ (and as a result between vectors $\mathbf{B_iP}$ and $\mathbf{B_iI_i}$ – Fig. 3), $\bar{\mathbf{d}}_{BiP}$, $\mathbf{v}_i$ and ω_i being defined at (2) and (5). It should be mentioned that the distance between point P and I_i is equal to $\gamma_i d_i$.

This equation is the basic result of the present paper, which shows that, for a given set of external force and moment applied on the platform, the reactions in passive joints depend not only on the pressure angle but also the position of the instantaneous centre of rotation of the platform. This property has not been rigorously formulated and demonstrated before. It allows not only giving a qualitative evaluation of the kinetostatic properties of the parallel manipulators and reducing the computational time but also disclosing the geometrical interpretation of the problem: from the equation (8), it can be shown that the mechanical system under study can be instantaneously replaced by a virtual cantilever attached to the ground at I_i (Fig. 3) lying on a virtual point contact at B_i, of which direction is parallel to the vector $\mathbf{R_i}$. The external force $\mathbf{f}$ is applied on the point P of the cantilever.

As α_i and d_i are criterion used for the kinetostatic design of robots [6, 7], it is of interest to find their boundaries with respect to some design requirements. In order to avoid the breakdown of the studied joint, technological requirements imply that the admissible value of R_i should not be superior to a given value R_{adm}, i.e. $R_{i\max} \le R_{adm}$. Thus, we would like to find α_i and d_i, i.e. the parameters of the equivalent cantilever system, for which this inequality is respected. Introducing (8) into the last inequality leads to:

$$f\sqrt{1 + (b_i/d_i)^2 - 2\cos\beta_i\, b_i/d_i} \le R_{adm}\cos\alpha_i - \left|m\right|/d_i. \qquad (9)$$

Please note that, as by definition, f, cos α_i, d_i and R_{adm} have positive values, a necessary condition for the existence of (9) is:

$$0 \le R_{adm}\cos\alpha_i - \left|m\right|/d_i \;\Rightarrow\; \frac{\left|m\right|}{R_{adm}\cos\alpha_i} \le d_i. \qquad (10)$$

If not, the left term of (9) will always be superior to R_{adm}. Let us now square the left and right sides of equation (9) and multiply them by d_i^2:

$$f^2\left(d_1^2+b_1^2-2\cos\beta_1\, b_1 d_1\right)\le d_1^2\left(R_{adm}\cos\alpha_1\right)^2+\ldots \\ \ldots m^2-2\,d_1\left|m\right|R_{adm}\cos\alpha_1 \quad (11)$$

The obtained expression can be rewritten as:

$$0\le p_i(d_i)\,, \quad (12)$$

where, $p_i(d_i)=u_i\,d_i^2+v_i\,d_i+w_i$, $u_i=R_{adm}^2\cos^2\alpha_i-f^2$, $v_i=-2\left(\left|m\right|R_{adm}\cos\alpha_i-\cos\beta_i\,b_i f^2\right)$, $w_i=m^2-f^2b_i^2$.

The inequality (12) has different solutions, depending on the vanishing and signs of terms u_i, v_i and w_i. There are three main cases $u_i > 0$, $u_i < 0$ and $u_i = 0$.

Let us consider these cases.

A. $u_i > 0$

$u_i > 0$ implies that $f < R_{adm}\cos\alpha_i$. In this case, the polynomial p_i has got two roots but only one corresponds to the real mechanism, i.e. to a solution of (9). The other root is solution of:

$$-f^2d_1^2\gamma_1^2\le d_1^2\left(R_{adm}\cos\alpha_1\right)^2+m^2-2\,d_1\left|m\right|R_{adm}\cos\alpha_1 \quad (13)$$

In order to obtain a root of (12) with physical values, it is necessary that the condition $v_i^2-4u_iw_i\ge 0$ should be respected, i.e

$$\left(R_{adm}^2f^2b_i^2\right)\cos^2\alpha_i-2\left(\left|m\right|R_{adm}\cos\beta_i\,b_if^2\right)\cos\alpha_i \\ \ldots-\sin^2\beta_i\,b_i^2f^4+f^2m^2\ge 0 \quad (14)$$

Developing and simplifying, it can be shown that this polynomial in cos α_i has roots with real values if and only if:

$$R_{adm}^2\sin^2\beta_i\,b_i^2f^4w_i\le 0\,. \quad (15)$$

For the analysis of this inequality, two following cases must be considered: $w_i \le 0$ and $w_i > 0$.

A1. $w_i > 0$

The condition $w_i > 0$ implies that $\left|m\right| > f\,b_i$. Here, (14) has no real roots, i.e. (14) is true for any value of α_i. Thus, the condition for (9) to be true is that

$$d_i\ge\max\left(\left(d_i\right)_1,\left|m\right|/\left(R_{adm}\cos\alpha_i\right)\right). \quad (16).$$

where $\left(d_i\right)_1=\left(-v_i+\sqrt{v_i^2-4u_iw_i}\right)\Big/2u_i$ is the root of (12) solution of (9).

A2. $w_i \le 0$

The condition $w_i \le 0$ implies that $\left|m\right| \le f\,b_i$. (14) is true if its roots are bounded by

$$\cos\alpha_i\ge\frac{\left|m\right|\cos\beta_i+\left|\sin\beta_i\right|\sqrt{f^2b_i^2-m^2}}{R_{adm}b_i} \quad (17a)$$

or

$$\cos\alpha_i\le\frac{\left|m\right|\cos\beta_i-\left|\sin\beta_i\right|\sqrt{f^2b_i^2-m^2}}{R_{adm}b_i} \quad (17b)$$

After mathematical simplifications, it can be proven that if (17b) is true, then,

$$\cos\alpha_i\le\frac{\left|m\right|}{R_{adm}b_i}\le\frac{f}{R_{adm}}\,. \quad (18)$$

which is in contradiction with $u_i > 0$. Therefore, the only condition for (14) to be true is that

$$\cos\alpha_i\ge\max\left(\frac{\left|m\right|\cos\beta_i+\left|\sin\beta_i\right|\sqrt{f^2b_i^2-m^2}}{R_{adm}b_i},\frac{f}{R_{adm}}\right) \quad (19)$$

However, it can be demonstrated that, for $u_i > 0$ and $w_i \le 0$

$$\frac{\left|m\right|\cos\beta_i+\left|\sin\beta_i\right|\sqrt{f^2b_i^2-m^2}}{R_{adm}b_i}\le\frac{f}{R_{adm}}\,. \quad (20)$$

Thus (19) implies that $u_i > 0$, which is true. Then, (14) is always true is this section. As a result, the only condition for (9) to be true is (16).

B. $u_i < 0$

$u_i < 0$ implies that $f > R_{adm}\cos\alpha_i$. Introducing this into (9) leads to $0 \le \gamma_i \le 1$, i.e. the cantilever allows decreasing the applied force **f**. Here also, two cases should be studied: $w_i \le 0$ and $w_i > 0$.

B1. $w_i > 0$

If $w_i > 0$, i.e. $\left|m\right| > f\,b_i$, from (10) it can be shown that:

$$\frac{fb_i}{R_{adm}\cos\alpha_i}<\frac{\left|m\right|}{R_{adm}\cos\alpha_i}\le d_i\,. \quad (21)$$

As in section II.B $u_i < 0$, which is equivalent to $R_{adm}\cos\alpha_i < f$, from (21) it comes

$$b_i<\frac{fb_i}{R_{adm}\cos\alpha_i}\text{, thus } b_i<d_i\,. \quad (22)$$

If (22) is true, the expression of γ_i at (8) is bounded by

$$\gamma_i\ge\frac{\left|b_i-d_i\right|}{d_i}=\frac{d_i-b_i}{d_i}>0\,. \quad (23)$$

Introducing (23) into (9), and as $\left|m\right| > f\,b_i$, it comes that:

$$\frac{f\left(d_i-b_i\right)+fb_i}{d_i}=f<\frac{f\left(d_i-b_i\right)+\left|m\right|}{d_i}\le R_{adm}\cos\alpha_i\,. \quad (24)$$

Thus,

$$f<R_{adm}\cos\alpha_i\text{, or equivalently } u_i>0, \quad (25)$$

which is impossible in section 2.2.

B2. $w_i \le 0$

If $w_i \le 0$, i.e. $\left|m\right| \le f\,b_i$, it could be shown after several mathematical simplifications that (14) is true if and only if

$$\frac{f}{R_{adm}}>\cos\alpha_i\ge\frac{\left|m\right|\cos\beta_i+\left|\sin\beta_i\right|\sqrt{f^2b_i^2-m^2}}{R_{adm}b_i}\,. \quad (26)$$

<table>
<tr><td></td><td>$|m| > fb_i$</td><td colspan="5">$|m| < fb_i$</td><td colspan="2">$|m| = fb_i$</td></tr>
<tr><td>$\frac{f}{R_{adm}} < \cos\alpha_i$</td><td colspan="8">$d_i \geq \max\left((d_i)_1, \frac{|m|}{R_{adm}\cos\alpha_i} \right)$</td></tr>
<tr><td>$\frac{f}{R_{adm}} > \cos\alpha_i$</td><td>N/A</td><td colspan="8">$\cos\alpha_i \geq \frac{|m|\cos\beta_i + |\sin\beta_i|\sqrt{f^2 b_i^2 - m^2}}{R_{adm} b_i}$, $\max\left(\frac{|m|}{R_{adm}\cos\alpha_i}, \frac{b_i}{2\cos\beta_i} \right) \leq d_i \leq (d_i)_2$</td></tr>
<tr><td rowspan="2">$\frac{f}{R_{adm}} = \cos\alpha_i$</td><td rowspan="2">N/A</td><td>$v_i > 0$</td><td>$v_i < 0$</td><td>$v_i = 0$</td><td>$v_i > 0$</td><td>$v_i < 0$</td><td colspan="2">$v_i = 0$</td></tr>
<tr><td>$d_i \geq \max\left(\frac{|m|}{R_{adm}\cos\alpha_i}, \frac{-w_i}{v_i} \right)$</td><td>N/A</td><td>N/A</td><td>$d_i \geq \frac{|m|}{R_{adm}\cos\alpha_i}$</td><td>N/A</td><td colspan="2">$d_i \geq b_i$, for $\beta_i = 0$</td></tr>
</table>

TABLE 1. Conditions for limiting the maximal values of the revolute joint linked to the platform.

Once this condition is achieved, the condition for (9) to be true is that

$$\max\left(\frac{|m|}{R_{adm}\cos\alpha_i}, \frac{b_i}{2\cos\beta_i} \right) \leq d_i \leq (d_i)_2 . \quad (27)$$

where $(d_i)_2 = \left(-v_i - \sqrt{v_i^2 - 4u_i w_i} \right) \Big/ 2u_i$ is the root of (12) solution of (9).

C. $u_i = 0$

We have to analyze one last case: $u_i = 0$, i.e. $\cos\alpha_i = f / R_{adm}$. Here also, this condition leads to $0 \leq \gamma_i \leq 1$, i.e. the cantilever allows decreasing the applied force **f**. In such a case, the solution of (12) is solution of $0 \leq v_i d_i + w_i$ with $v_i = 2f\left(\cos\beta_i b_i f - |m|\right)$ and $w_i = m^2 - f^2 b_i^2$.

Three cases will appear: $v_i > 0$, $v_i < 0$ and $v_i = 0$.

C1. $v_i > 0$

In this case, $R_{i\max} \leq R_{adm}$ can be satisfied if and only if

$$\frac{-w_i}{v_i} = \frac{f^2 b_i^2 - m^2}{2f\left(\cos\beta_i b_i f - |m|\right)} \leq d_i . \quad (28)$$

C2. $v_i < 0$

In this case, $R_{i\max} \leq R_{adm}$ can be satisfied if and only if

$$0 \leq d_i \leq \frac{-w_i}{v_i} = \frac{f^2 b_i^2 - m^2}{2f\left(\cos\beta_i b_i f - |m|\right)} . \quad (29)$$

As in section 2.2.1, the condition $w_i > 0$ is not compatible with the fact that $u_i = 0$. For $w_i \leq 0$:

$$\frac{f^2 b_i^2 - m^2}{2f\left(\cos\beta_i b_i f - |m|\right)} \leq 0 . \quad (30)$$

Therefore, if $v_i < 0$, the only condition is that (10) should be respected.

C3. $v_i = 0$

Condition (12) can be satisfied if and only if $w_i \geq 0$. But, as previously, $w_i > 0$ is not compatible with the fact that $u_i = 0$. Therefore, it exist only one possible case, $w_i = 0$, i.e. $fb_i = m$.

In table 1 are summarized all conditions for obtaining $R_{i\max} \leq R_{adm}$. It should be mentioned that for planar parallel robots, the reactions in the other joints that are not linked to the platform can be found using linear relationships with respect to $R_{i\max}$ (not detailed here).

Let us now consider an illustrative example.

III. Illustrative example

In this part, it is studied the effort transmission in a 3-*R*<u>*R*</u>*R* parallel manipulator (Fig. 2), with actuated joints located at C_i (represented in grey) having the following characteristics:

- points A_1, A_2 and A_3 and points B_1, B_2 and B_3 form equilateral triangles
- circumcircle of $A_1A_2A_3$ of radius $r_b = 0.35$ m
- circumcircle of $B_1B_2B_3$ of radius $r_p = 0.1$ m
- links length $l_{AiCi} = l_{CiBi} = 0.4$ m

For this robot, it is known that the directions of the forces $\mathbf{R_i}$ in the passive joints are directed along the vectors $\mathbf{A_iB_i}$ (Fig. 2) [5]. Moreover, its Type 2 singular configurations appears when [5]:

- the orientation of the platform is equal to 0 or 180 deg, for any position of the platform centre
- when the platform centre, for a given orientation ϕ, is located on a circle C centred in O of which radius is equal to $\sqrt{r_b^2 + r_p^2 - 2r_b r_p \cos\phi}$.

As a result, we will study the effort transmission in the passive joints of the robot in workspaces delimited by circles C..

For 3-$R\underline{R}R$ robots, it can be shown that the matrix $\mathbf{A}^T$ expressed at point B_i is equal to [5]:

$$\mathbf{A}^T = \begin{bmatrix} \mathbf{R_1} & \mathbf{R_2} & \mathbf{R_3} \end{bmatrix} = \begin{bmatrix} \mathbf{f_1} & \mathbf{f_2} & \mathbf{f_3} \\ m_1 & m_2 & m_3 \end{bmatrix} \tag{31}$$

with

$$\mathbf{f}_i^T = \begin{bmatrix} -\sin q_i & \cos q_i \end{bmatrix}$$

and, if $B_i = B_1$ then

$$m_1 = 0$$

$$m_2 = \sqrt{3} r_p \begin{bmatrix} -\sin\phi \\ \cos\phi \end{bmatrix}^T \mathbf{f_2} \tag{32a}$$

$$m_3 = \sqrt{3} r_p \begin{bmatrix} -\sin(\pi/3+\phi) \\ \cos(\pi/3+\phi) \end{bmatrix}^T \mathbf{f_3}$$

if $B_i = B_2$ then

$$m_1 = \sqrt{3} R_p \begin{bmatrix} -\sin(\phi+\pi) \\ \cos(\phi+\pi) \end{bmatrix}^T \mathbf{f_1}$$

$$m_2 = 0 \tag{32b}$$

$$m_3 = \sqrt{3} R_p \begin{bmatrix} -\sin(2\pi/3+\phi) \\ \cos(2\pi/3+\phi) \end{bmatrix}^T \mathbf{f_3}$$

if $B_i = B_3$ then

$$m_1 = \sqrt{3} R_p \begin{bmatrix} -\sin(\phi+4\pi/3) \\ \cos(\phi+4\pi/3) \end{bmatrix}^T \mathbf{f_1}$$

$$m_2 = \sqrt{3} R_p \begin{bmatrix} -\sin(-\pi/3+\phi) \\ \cos(-\pi/3+\phi) \end{bmatrix}^T \mathbf{f_2} \tag{32c}$$

$$m_3 = 0$$

The pressure angles and the distances to the instantaneous centre of rotation can be computed using the geometric representation shown in Fig. 2. In Fig. 4 are presented the variations of the joint reactions at point B_1 within the workspace for several platform orientations ϕ, for f = 100 N and m = 5 Nm. Indeed, for this kind of robot, it can be shown that the reactions inside of the whole joints of leg i are equal to R_i. Therefore studying the value of $R_{i\max}$ at B_i allows having good information about the force transmission inside of leg i.

It can be observed that, the closer to Type 2 singularities, the higher the joint reaction. Moreover, the lowest values of the joint reactions appear in zones close to the workspace centre.

Let us now compute the force workspaces of the manipulator. The method consists in discretising the workspace using polar coordinates (r, θ). For one given angle θ, the algorithm tests for all rising values of r that the manipulator can support the applied wrench (see table 1). In the case where the manipulator cannot support the

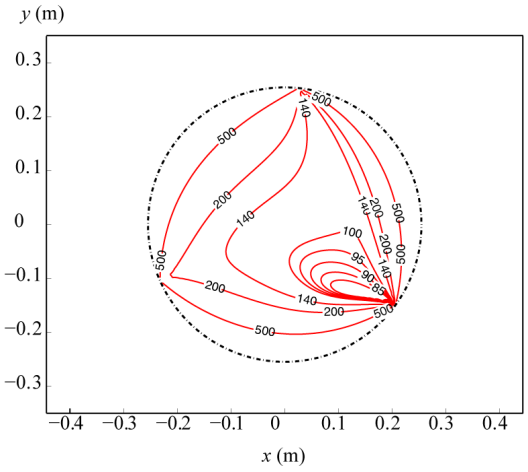

(a) ϕ =15 deg

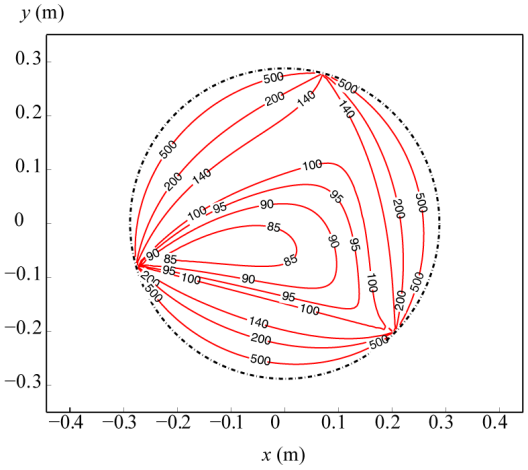

(b) ϕ =45 deg

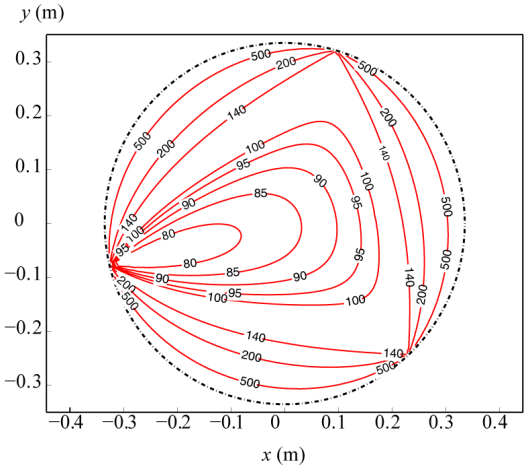

(c) $\phi = \cos^{-1}(r_p/r_b) \approx 73$ deg

Fig. 4. Variations of the joint reactions (in Newtons) at B_1 within the workspace for several platform orientations ϕ, for f = 100 N and m = 5 Nm.

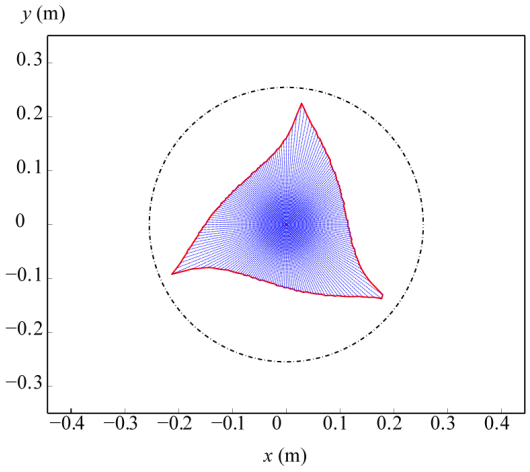

(a) ϕ =15 deg

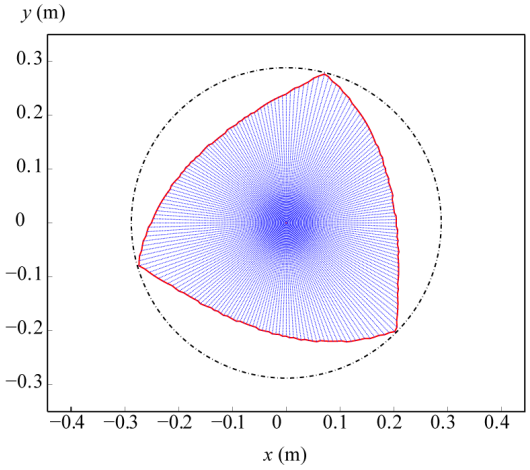

(b) ϕ =45 deg

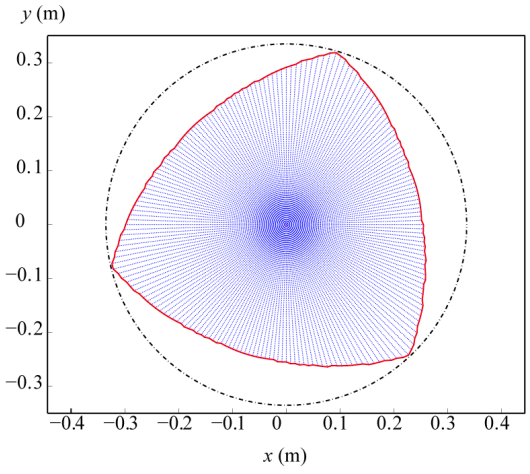

(c) $\phi = \cos^{-1}(r_p/r_b) \approx 73$ deg

Fig. 5. Constant orientation workspace for several platform orientations ϕ, for f = 100 N and m = 5 Nm and R_{adm} = 200 N.

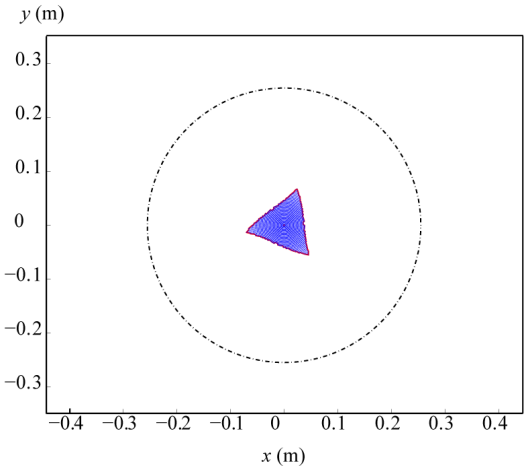

(a) ϕ =15 deg

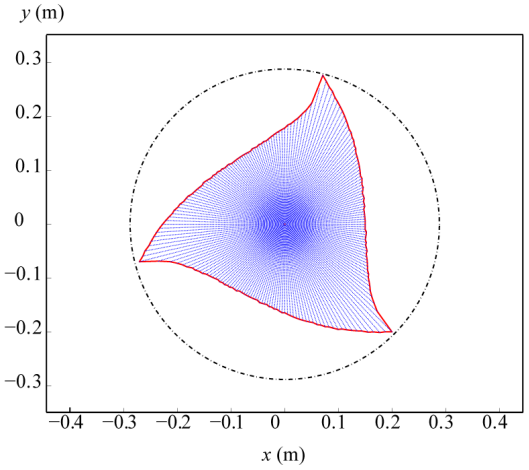

(b) ϕ =45 deg

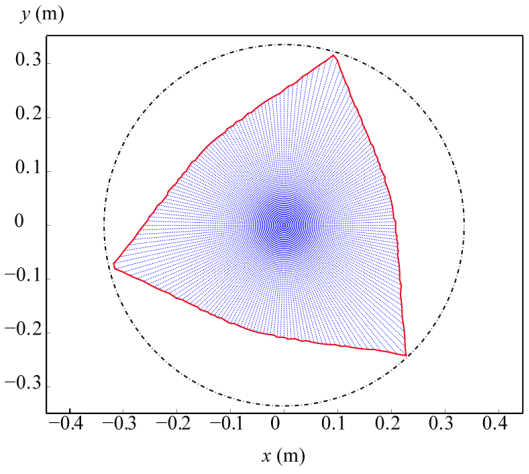

(c) $\phi = \cos^{-1}(r_p/r_b) \approx 73$ deg

Fig. 6. Constant orientation workspace for several platform orientations ϕ, for f = 100 N and m = 5 Nm and R_{adm} = 130 N.

applied wrench, the boundary of the force workspace is defined by the previous computational point.

In the following of this example, it is considered that the maximal admissible value R_{adm} of the reactions of the revolute joints should be equal to 200 N in one case, and to 130 N in a second case. The same wrench as previously is applied on the platform, i.e. a force of norm f = 100 N, and a moment of norm m = 5 Nm. The shape of the force workspace, for one given assembly mode and for several values of platform orientation ϕ and of R_{adm} is shown in Figs. 5 and 6.

It can be observed that, the smaller ϕ, i.e. the closer from the orientation for which the robot is in singular configuration for any position of the platform centre, the smaller the workspace.

V. Conclusions

In this paper has been presented a method that allows computing the maximal efforts in the joints of planar parallel manipulators. Trivial solution of this task could be the calculation of joint reactions for several values of the external wrench. However such a solution is very time consuming and do not give any quantitative or geometrical evaluation of the effort transmission. In the present paper a new approach has been developed, which has shown that for given external force and moment applied on the platform, the reactions in passive joints depend not only on the pressure angle but also the position of the instantaneous centre of rotation of the platform. This is the first time that such a kinetostatic property is rigorously formulated and clearly demonstrated. The obtained results allow expanding the knowledge about the criteria for measuring closeness to singularity and to avoid the mechanical breakdown by exceeding the admissible values of reactions in passive joints of planar parallel manipulators. In this aim, the optimal boundaries for the values of the pressure angle and of the distance to the instantaneous centre of rotation are computed. The 3-*RRR* robot has been studied as an illustrative example. Its effort transmission has been studied as well as its maximal reachable workspace.

References

[1] Gosselin, C.M., Angeles, J. Singularity analysis of closed-loop kinematic chains. IEEE Transactions on Robotics and Automatics, 6(3): 281–290, 1990.

[2] Basu, D. and Ghosal A. Singularity analysis of platform-type multi-loop spatial mechanisms. Mechanism and Machine Theory, 32(3):375–389, 1997.

[3] Merlet, J.-P. Singular configurations of parallel manipulators and grassmann geometry. The international Journal of Robotics Research, 8(5):45–56, 1989.

[4] Zlatanov, D., Bonev, I.A., Gosselin, C. M. Constraint singularities of parallel mechanisms. IEEE International Conference on Robotics and Automation, Washington, D.C., USA, May 11-15, 2002.

[5] Bonev, I.A., Zlatanov, D., Gosselin, C.M. Singularity analysis of 3-DOF planar parallel mechanisms via screw theory. ASME Journal of Mechanical Design, 125(3):573–581, 2003.

[6] Alba-Gomez, O., Wenger, P. and Pamanes, A. Consistent kinetostatic indices for planar 3-DOF parallel manipulators, application to the optimal kinematic inversion. Proceedings of the ASME 2005 IDETC/CIE Conference, September 24-28, Long Beach, California, 2005.

[7] Arakelian, V., Briot, S., Glazunov, V. Increase of singularity-free zones in the workspace of parallel manipulators using mechanisms of variable structure. Mechanism and Machine Theory, 43(9):1129–1140, 2008.

[8] Hubert J. and Merlet J.-P. Static of parallel manipulators and closeness to singularity. Journal of Mechanisms and Robotics, 1(1), February 2009.

[9] Nenchev, D.N., Bhattacharya, S., Uchiyama, M. Dynamic analysis of parallel manipulator under the singularity-consistent parameterization. Robotica, 4(4):375–384, 1997.

[10] Briot, S. and Arakelian, V. Optimal force generation of parallel manipulators for passing through the singular positions. International Journal of Robotics Research, 27(8):967–983, 2008.

[11] Briot, S. and Arakelian, V. On the dynamic properties of rigid-link flexible-joint parallel manipulators in the presence of type 2 singularities. Journal of Mechanisms and Robotics, 2(2), 2010.

[12] Pottmann, H, Peternell, M. and Ravani, B. Approximation in line space: Applications in robot kinematics and surface reconstruction. Advances in Robot Kinematics: Analysis and Control, A. Lenarcic and M. Husty, Eds. Dordrecht, The Netherlands: Kluwer Academic Publishers, 1998, pp. 403-412.

[13] Wolf, A., and Shoham, M. Investigation of parallel manipulators using linear complex approximation. Journal of Mechanical Design, 125(3):564–572, September 2003.

[14] Lipkin H. and Patterson T. Geometrical properties of modelled robot elasticity: Part I – decomposition. Proceedings of the 1992 ASME Design Technical Conferences: 22nd Biennial Mechanisms Conference, vol. Robotics, Spatial Mechanisms, and Mechanical Systems, Scottsdale, AZ, September 1992, pp. 179–185.

[15] Lipkin H. and Patterson T. Geometrical properties of modelled robot elasticity: Part II - center of elasticity. Proceedings of the 1992 ASME Design Technical Conferences: 22nd Biennial Mechanisms Conference, vol. Robotics, Spatial Mechanisms, and Mechanical Systems, Scottsdale, AZ, September 1992, pp. 187–193.

[16] Gosselin, C.M. The optimum design of robotic manipulators using dexterity indices, Robotics and Autonomous Systems, 9(4):213–226, 1992.

[17] Gosselin, C.M. and Angeles, J. A global performance index for the kinematic optimization of robotic manipulators, Journal of Mechanical Design, 113(3):220–226, 1991.

[18] Briot, S., Pashkevich, A. and Chablat, D. Optimal technology-oriented design of parallel robots for high-speed machining applications. Proceedings of the 2010 IEEE International Conference on Robotics and Automation (ICRA 2010), May 3-8, 2010, Anchorage, Alaska, USA.